

Figure 13.1 Dependence of resistance to convective heat transfer r_H and resistance to radiative heat exchange r_R as a function of body size represented by the characteristic dimension of a cylinder d . The cylinder is assumed exposed in a wind tunnel where air and wall radiative temperatures are identical. The curves are calculated for wind speeds, V , of 1 m s^{-1} and 10 m s^{-1} . The right-hand axis shows the rate of heat transfer assuming a difference of 1 K between cylinder surface temperature and air/wall radiative temperature.

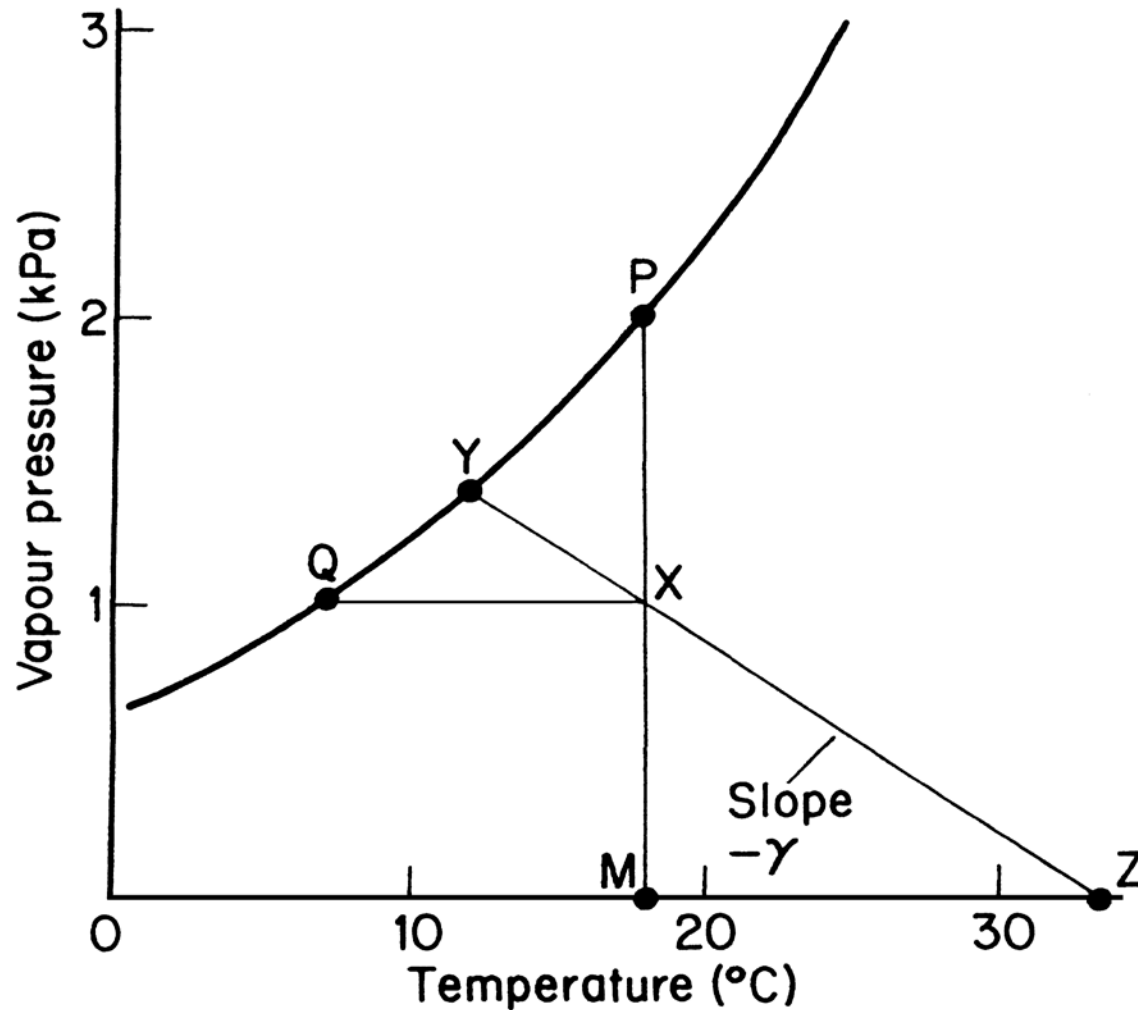


Figure 13.2 The relation between dry-bulb temperature, wet-bulb temperature, equivalent temperature, vapor pressure, and dew point. The point X represents air at 18 °C and 1 kPa vapor pressure. The line YXZ with a slope of $-\gamma$ gives the wet-bulb temperature from Y (12 °C) and the equivalent temperature from Z (33.3 °C). The line QX gives the dew-point temperature from Q (7.1 °C). The line XP gives the saturation vapor pressure from P (2.1 kPa).

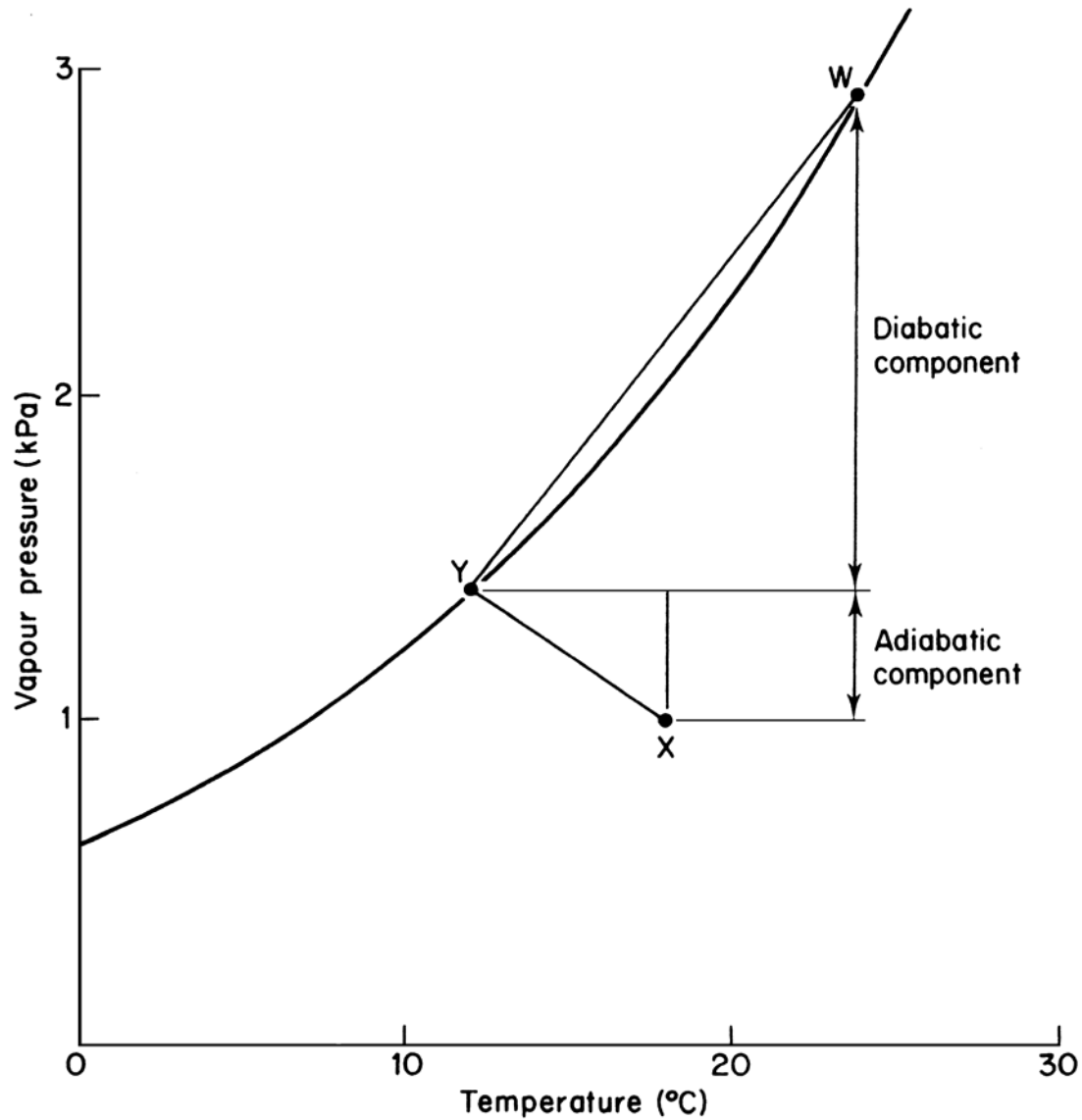


Figure 13.3 Basic geometry of the Penman Equation (from Monteith, 1981a). A parcel of air at X is cooled adiabatically to Y (cf. Figure 13.2) and heated diabatically to W. Corresponding quantities of latent heat are given in Eq. (13.26).

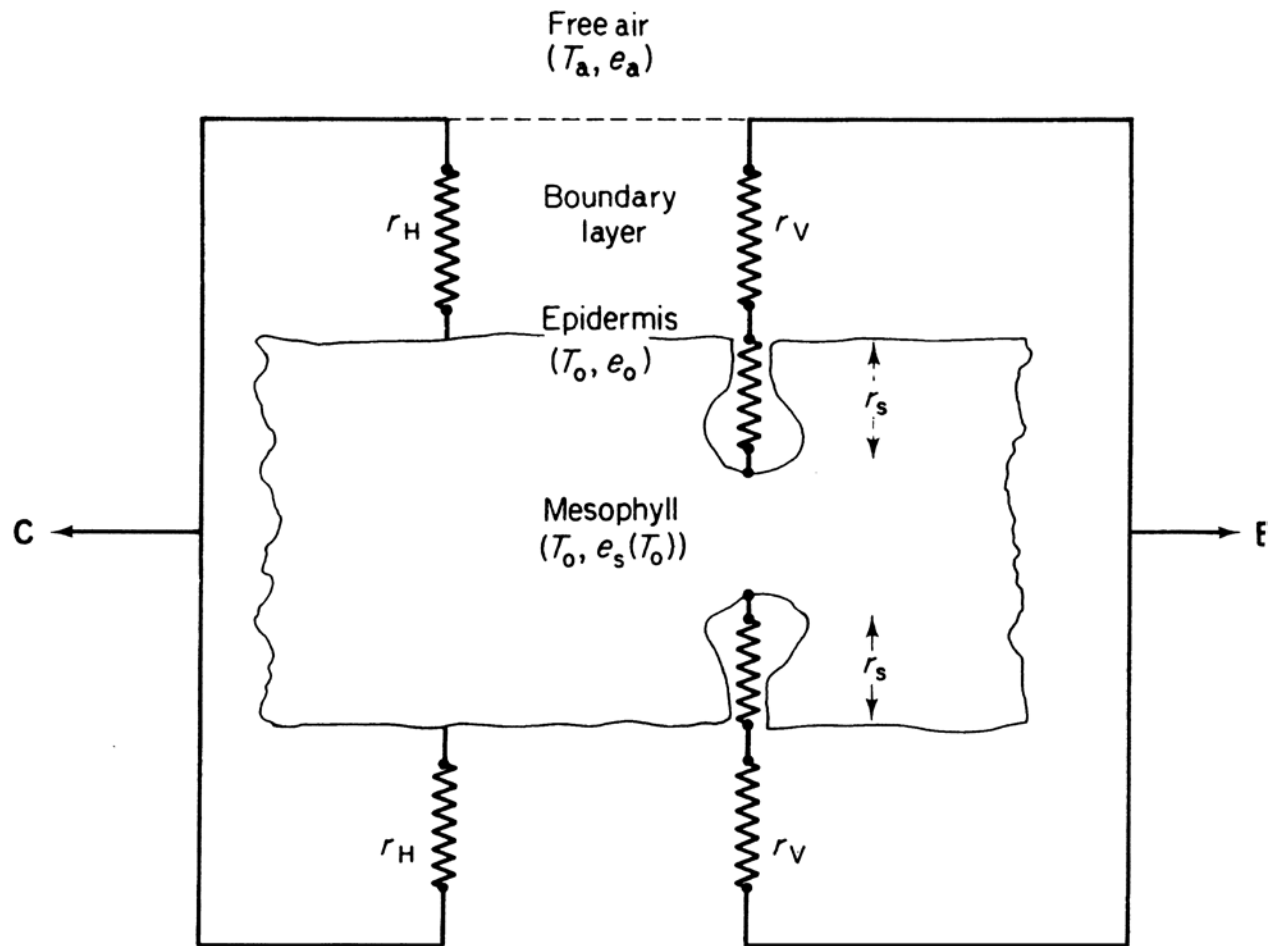


Figure 13.4 Electrical analog for transpiration from a leaf and leaf heat balance (see also Figure 11.8).

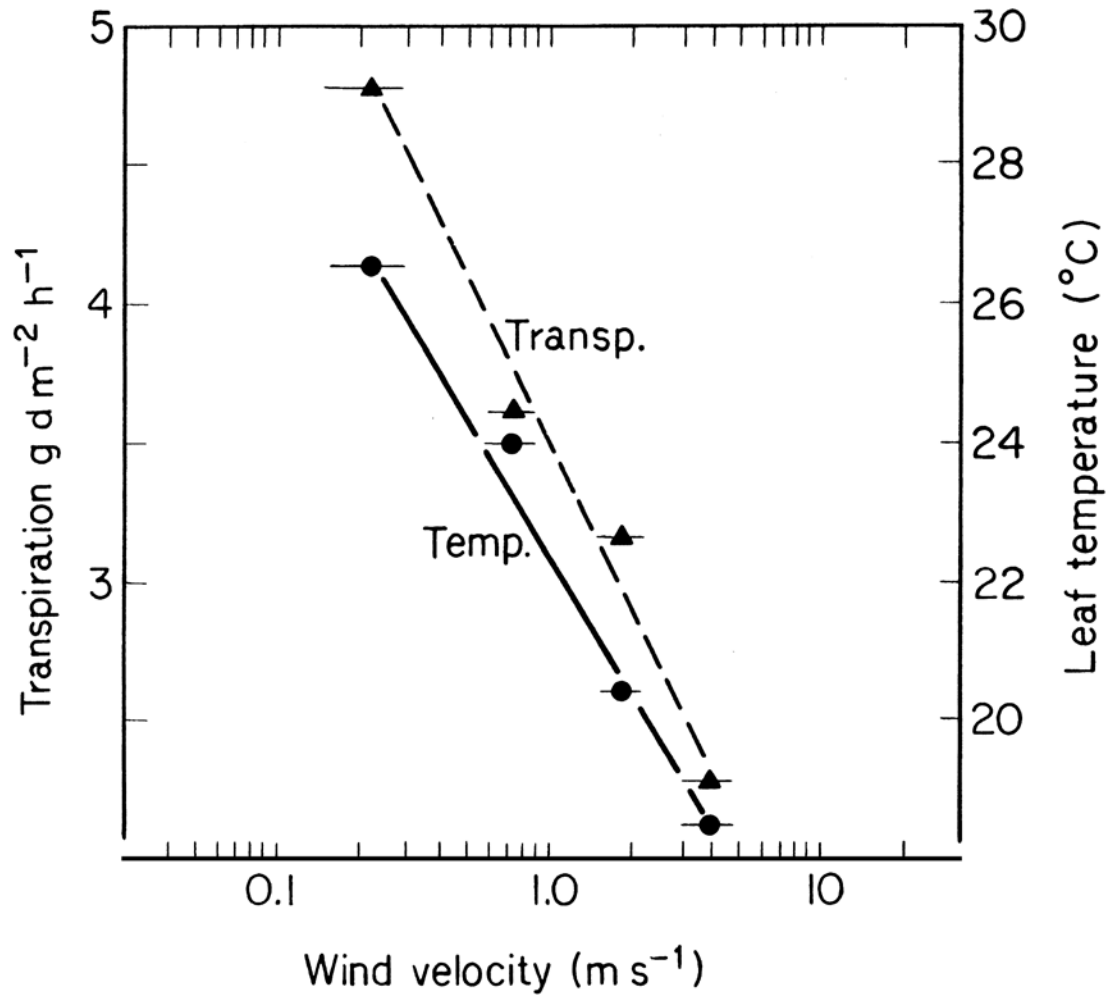


Figure 13.5 The change of transpiration rate and leaf temperature with windspeed for a *Xanthium* leaf exposed to radiation of 700 W m^{-2} at an air temperature of 15°C and 95% relative humidity. (From Mellor et al., 1964)

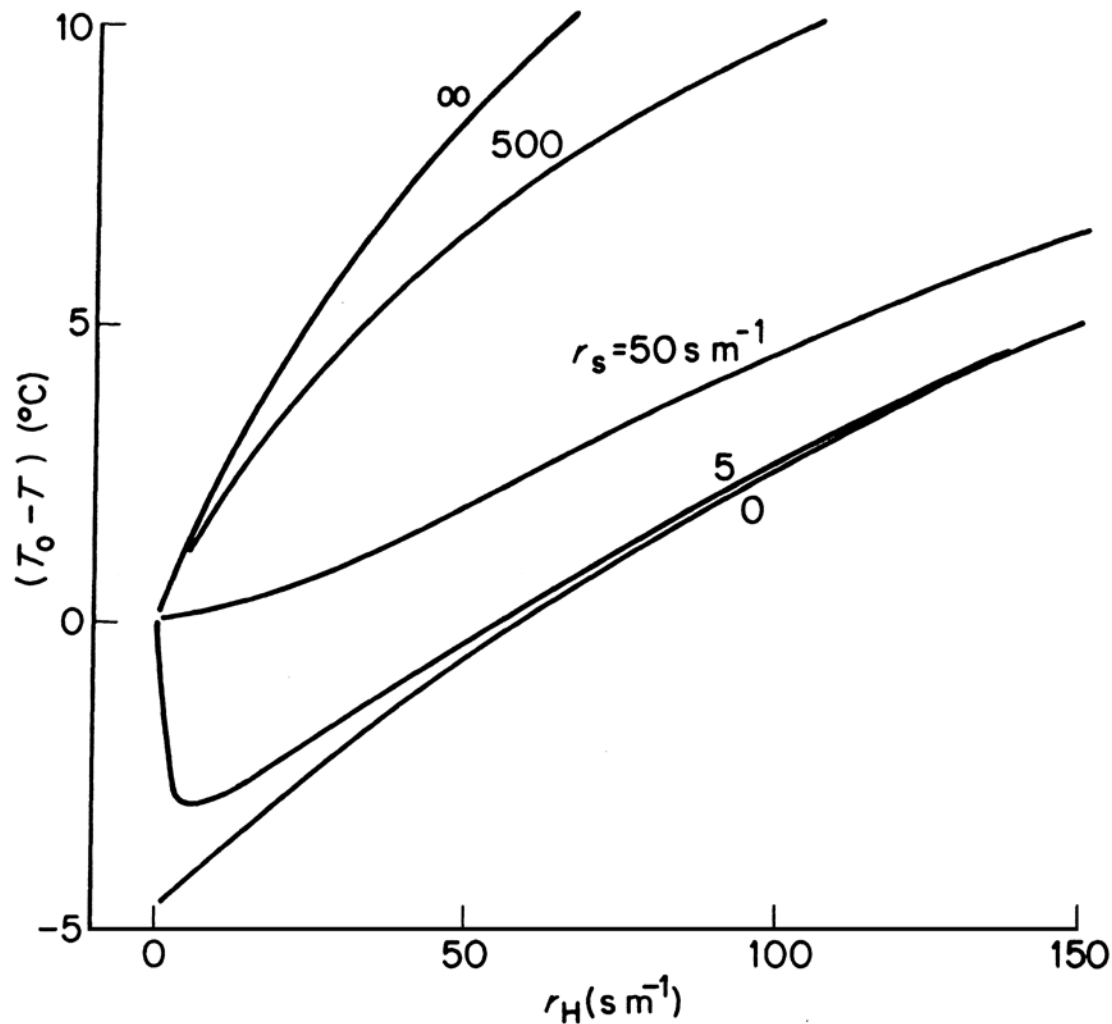


Figure 13.6 Predicted difference between surface and air temperature for an amphistomatous leaf in sunlight with specified boundary layer and stomatal resistances (for both laminae in parallel). Assumed microclimate: $R_{ni} = 300 \text{ W m}^{-2}$, $T = 20^{\circ}\text{C}$, saturation deficit 1 kPa (from Monteith, 1981b).

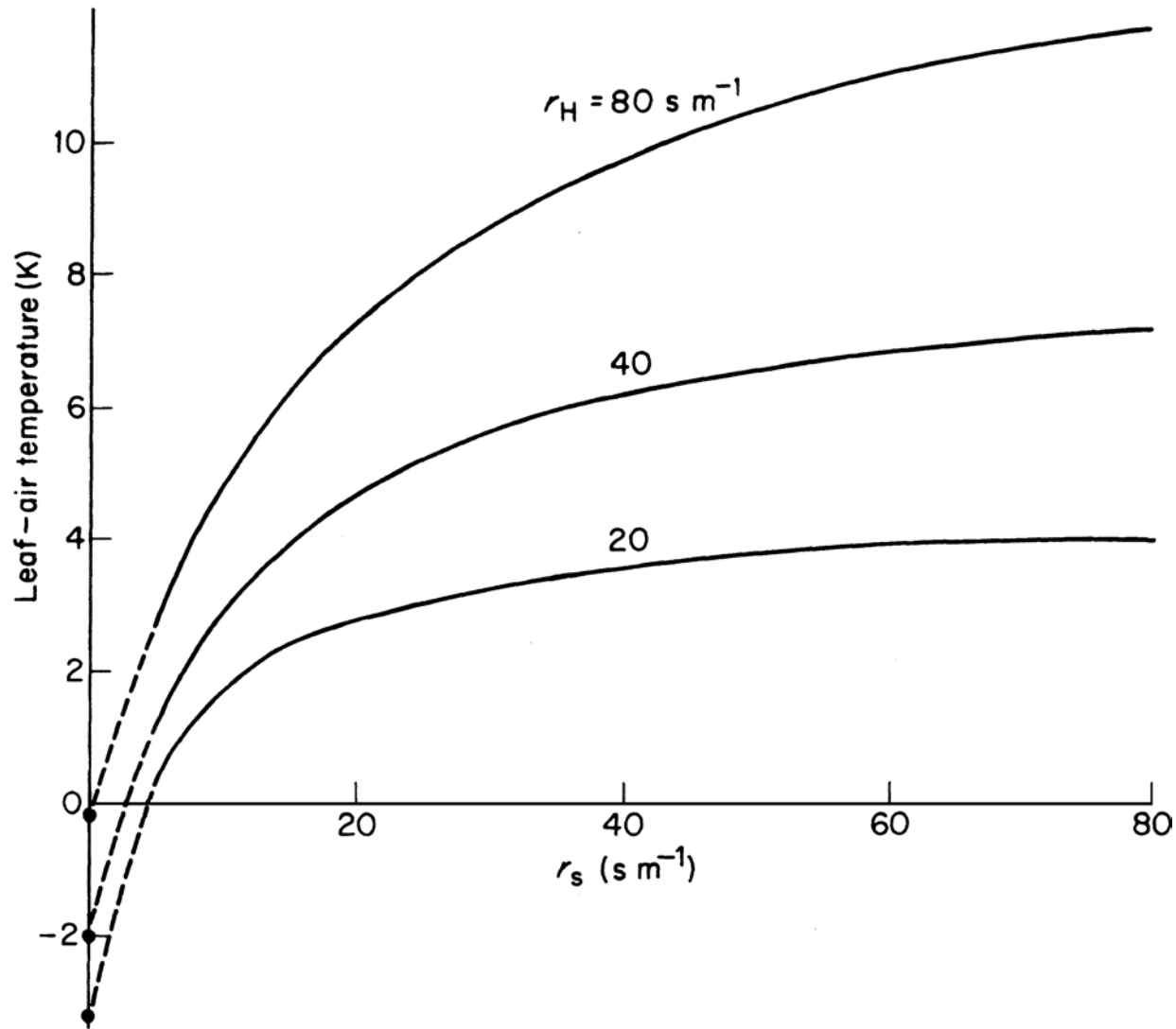


Figure 13.7 Excess of leaf over air temperature as a function of stomatal and aerodynamic resistances when $R_{ni} = 300 \text{ W m}^{-2}$, $D = 1 \text{ kPa}$, $T = 20^\circ \text{C}$ (see also Figure 13.6).

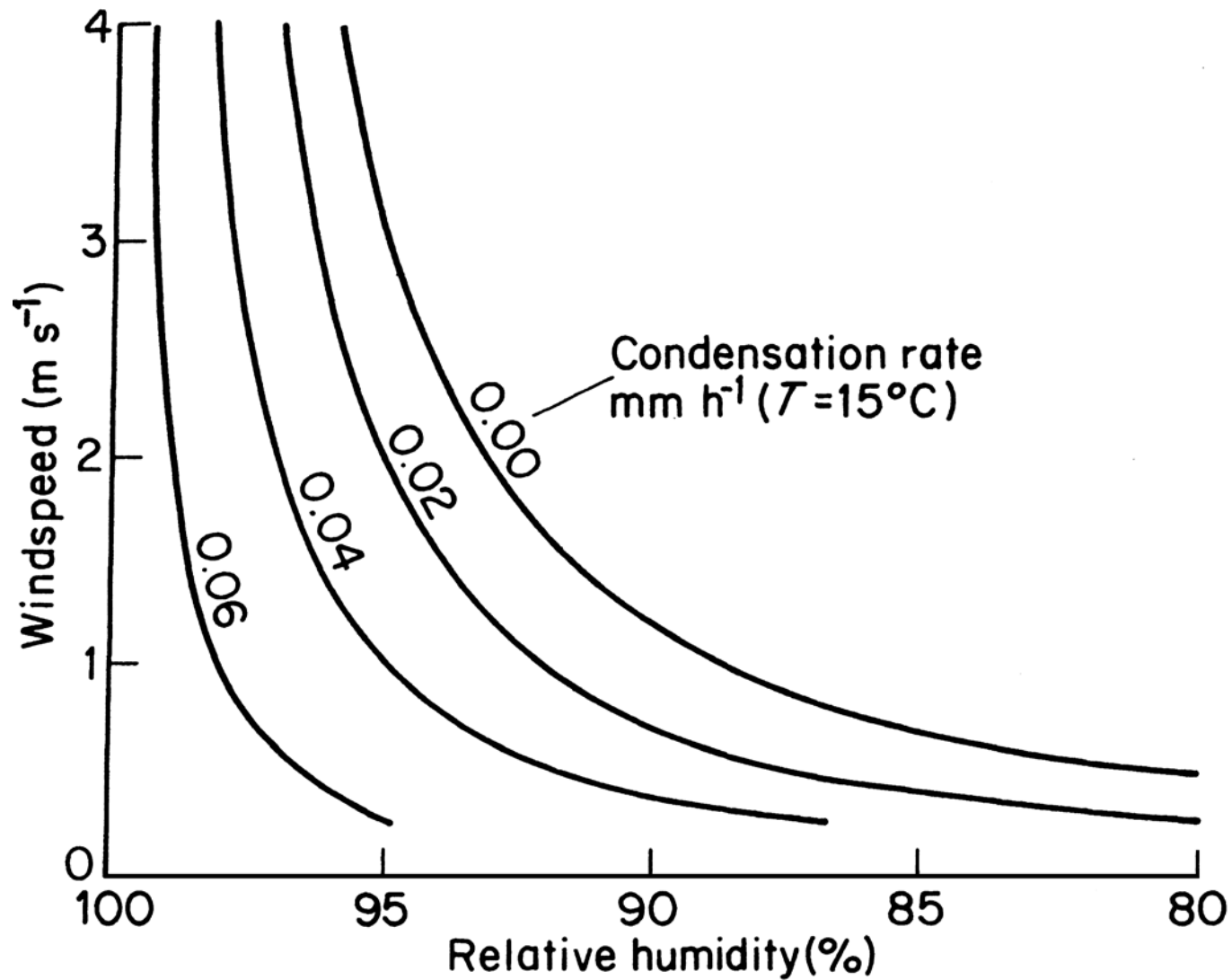


Figure 13.8 The rate of condensation on a horizontal plane exposed to a cloudless sky at night when the air temperature is 15°C , as a function of windspeed and relative humidity (from Monteith, 1981b).

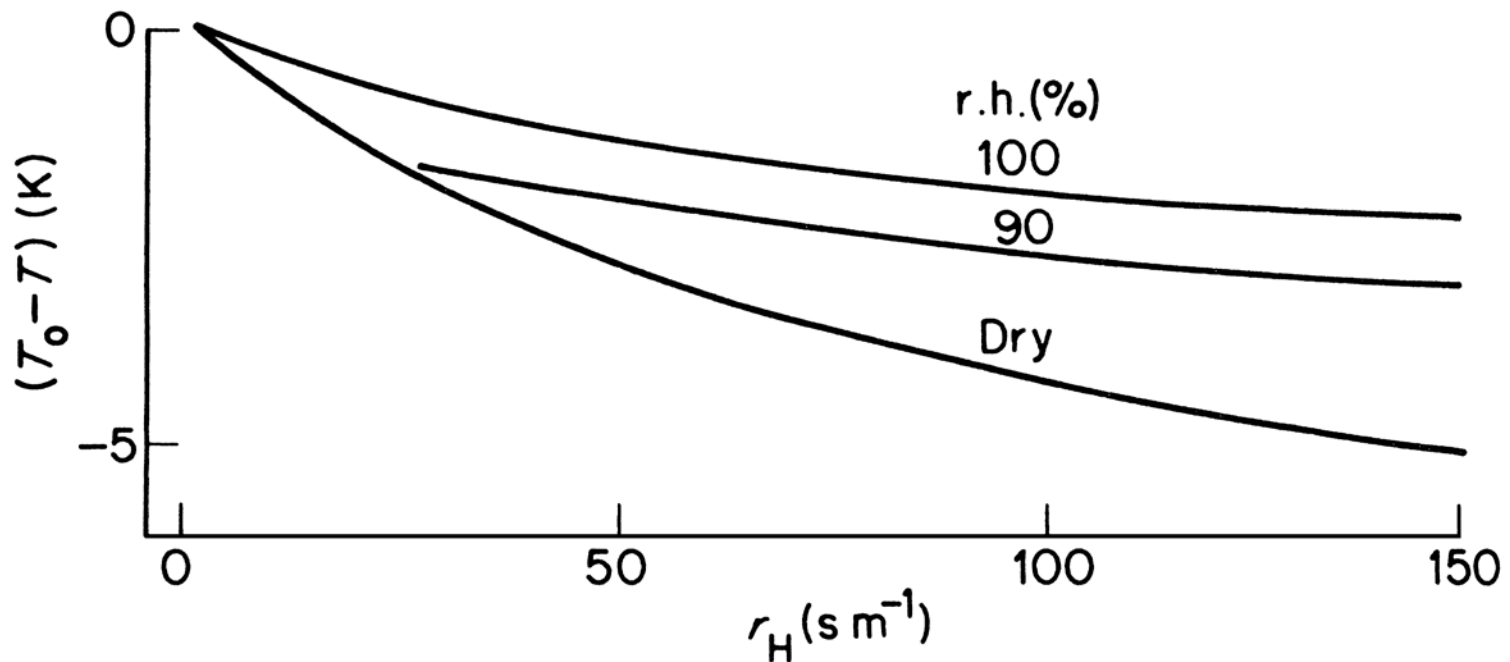


Figure 13.9 Predicted difference between surface and air temperature for a leaf with specified boundary layer resistance in the dark ($r_s = \infty$). Assumed microclimate: $R_n = -100 \text{ W m}^{-2}$; $T = 10^\circ \text{C}$. Dew formation occurs when relative humidity is 100% or 90%. The “dry” curve is appropriate when the relative humidity is too low to allow condensation (from Monteith, 1981b).



Figure 13.10 Hoar frost on leaves of *Helleborus corsicus*. Note the preferential formation of ice on the spikes. The exchange of heat and water vapor is faster round the edge of a leaf than in the center of the lamina because the boundary layer is thinner at the edge (p. 160). A faster exchange of heat implies that the spikes should be somewhat warmer than the rest of the leaf, i.e. closer to air temperature at night. A faster rate of mass exchange implies that the spikes should collect hoar frost faster than the center of the lamina when their temperature is below the frost-point temperature of the air (Courtesy of R.L. Milstein).

Table 13.1 Typical Minimum Canopy Resistances r_c for Various Vegetation Types (Based on Kelliher et al., 1995)

Vegetation type	r_c (s m ⁻¹)
Temperate grassland	60
Coniferous forest	50
Temperate deciduous forest	50
Tropical rain forest	80
Cereal crops	30
Broadleaved herbaceous crops	35

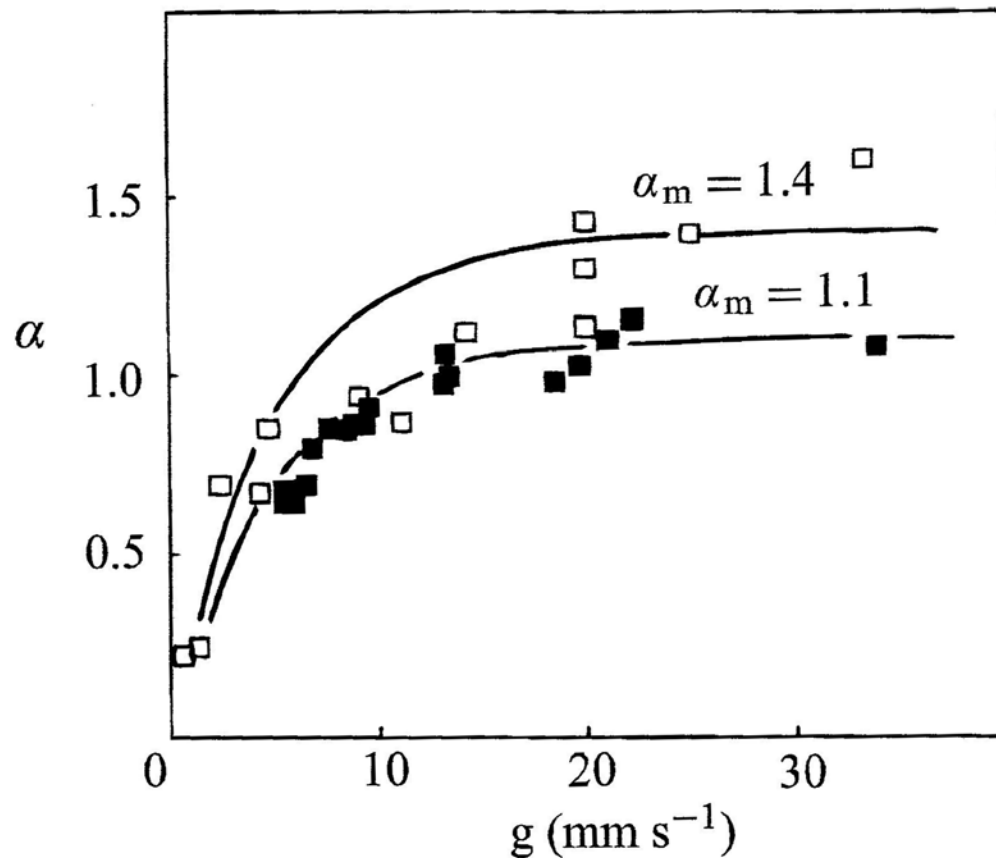


Figure 13.11 Increase in the Priestley-Taylor coefficient α with canopy conductance g ($= 1/r_c$). Filled squares are from De Bruin (1983); open points are from Monteith (1965). The curves are given by the empirical equation $\alpha = \alpha_m(1 - \exp(-g/g_c))$, with the scaling conductance $g_c = 5 \text{ mm s}^{-1}$ (In reality g_c probably depends on conditions at the top of the CBL). Curves with the scaling factor $\alpha_m = 1.1$ or 1.4 bracket the observed data (from Monteith, 1995b).

Table 13.2 Typical values of the Decoupling Coefficient Ω for unstressed leaves and canopies. (from Jarvis and Mcnaughton, 1986). For leaves, the characteristic dimension d (mm) is shown, and values are based on a windspeed of 1.0 m s^{-1} . For canopies, the value of r_a implicit in Ω is calculated for a reference level just above the vegetation surface

Species	d (mm)	Ω
Leaves		
<i>Tectona grandis</i> (Teak)	260	0.9
<i>Triplochiton scleroxylon</i> (Obeche)	200	0.6
<i>Malus pumila</i> (Apple)	60	0.3
<i>Fagus sylvatica</i> (Beech)	40	0.2
<i>Picea sitchensis</i> (Sitka spruce)	2	0.1
Canopies		
Alfalfa		0.9
Pasture, grassland		0.8
Potatoes, sugar beet, snap beans		0.7
Wheat, barley		0.6
Prairie		0.5
Cotton		0.4
Heathland		0.3
Pine forest		0.1